

Short Communication

The Corrosion Inhibition Effect of Thiourea for Q235 steel in Oxalic Acid Solution

Wei Du*, Zhongyu Yi, Tao Wang, Hengqiong Jia, Zhao Wei, Shaoliang Wu, Zhenping Shi

Metals and Chemistry Research Institute, China Academy of Railway Sciences Corporation Limited, Beijing, 100081, PR China.

*E-mail: Railwaydu@163.com

Received: 18 January 2022 / Accepted: 22 February 2022 / Published: 5 April 2022

This work is dedicated to exploring the optimum concentration and anti-corrosion mechanism of pickling agent that can effectively remove corrosion products of high-speed railway trains. A commonly used oxalic acid cleaning agent with thiourea was diluted to 5%, 10%, 15%, and 20%. Based on EIS and Tafel tests, we found that thiourea could provide efficient protection for Q235 steel when the diluted concentration was 5%. Meanwhile, thiourea was a modest and mixed corrosion inhibitor for Q235 steel in oxalic acid. SEM observation further proved the above conclusion. According to theoretical calculation, the high E_{HOMO} , μ , E_{binding} and low E_{LUMO} , ΔE values of thiourea stood for the excellent adsorption ability and supreme anti-corrosion performance.

Keywords: High-speed railway trains; Oxalic acid pickling agent; Corrosion inhibition; EIS; Theoretical calculation

1. INTRODUCTION

Trains are well known as a common means of transportation. Meanwhile, trains are the product of the steam age. It shortens travel time, brings convenience to people's travel, and becomes an indispensable part of people's lives. With the development of society and the progress of science and technology, traditional trains are replaced by high-speed railway trains, making people's travel more convenient. The running speed of high-speed railway trains is fast, up to 200-300 km/h. In addition, the running mileage of the high-speed railway train is also long, generally 2000 km a day. However, the fast speed of high-speed railway trains accelerates the corrosion of its steel components and makes the corrosion products more firm. In addition to passenger trains, freight trains also run on the same rails, complicating the composition of corrosion products [1-3]. It is necessary to develop pickling agents that can effectively remove corrosion products of high-speed railway trains [4, 5].

Oxalic acid is a common pickling agent for cleaning corrosion products on high-speed railway trains. Oxalic acid can easily remove the corrosion products and stains. It is worth noting that oxalic acid with strong acidic may also corrode the metal substrate after cleaning off the corrosion products and stains [6-8]. If the residual oxalic acid continues to corrode the metal parts of high-speed railway trains, the consequences will be disastrous. To reduce safety accidents and economic losses caused by corrosion of steel parts in high-speed railway trains, it is essential to add corrosion inhibitors to the oxalic acid pickling agent [9, 10].

Organic corrosion inhibitors normally contain unsaturated bonds (double and triple bonds) and heteroatoms (nitrogen, oxygen, sulfur, and phosphorus atom), facilitating the adsorption of organic molecules on the metal surface via physical and/or chemical force [11, 12]. In addition, organic corrosion inhibitors are more eco-friendly to humans and the environment than inorganic corrosion inhibitors (nitrite, phosphate, and chromate) [13]. Up to now, through the effort of researchers, a large number of organic corrosion inhibitors have been developed and applied. Qiang et al. explored the corrosion inhibition of two tetrazole compounds (BTA and BTTA) for copper in the sulfuric acid environment [14]. The experimental results showed that BTA and BTTA could give copper strong protection via the self-assembling anchored film, and the protective capacity was reinforced by the existence of the S atom. The corrosion inhibition mechanism of BTA and BTTA for copper was explained by quantum chemical calculations and molecular dynamics simulations. Tan et al. found that two food flavorants 2-isobutylthiazole (ITT) and 1-(1,3-Thiazol-2-yl)ethenone (TEO) could effectively inhibit the corrosion rate of X65 steel in sulfuric acid [10]. The corrosion inhibition efficiency of ITT and TEO was 70% and 89.9% when the added dose was 5 Mm. Fernandes et al. used a green synthesis of 1-benzyl-4-phenyl-1H-1,2,3-triazole (BPT) and investigated the anti-corrosion performance of BPT for A36 mild steel in an acidic medium [15]. Based on AFM research, the authors demonstrated satisfactory anti-corrosion ability of BPT for mild steel.

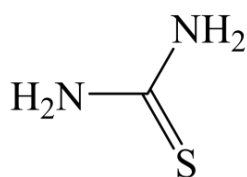


Figure 1. Chemical structure of thiourea.

Thiourea ($\text{CH}_4\text{N}_2\text{S}$) is an organic sulfur-containing compound commonly used to treat hyperthyroidism and manufacture drugs. The chemical structure of thiourea is shown in Fig. 1. Clearly, thiourea consists of two N atoms, one S atom, and an unsaturated double bond, which facilitates the adsorption of thiourea on the metal surface and protects the metal. To the best of our knowledge, no one has studied the corrosion inhibition effect of thiourea in oxalic acid pickling agent for Q235 steel so far. In this study, we diluted the commonly used high-speed railway trains pickling agent, which contained oxalic acid and thiourea. Based on the electrochemical impedance spectroscopy (EIS), the potentiodynamic polarization curve, scanning electron microscope (SEM), and theoretical calculation, the anti-corrosion performance of thiourea for Q235 steel in oxalic acid was explored carefully. There

is no doubt that this work will contribute to exploring the corrosion inhibition mechanism of organic corrosion inhibitors for the metal in oxalic acid. Meanwhile, this work promotes the practical application of organic corrosion inhibitors in the oxalic acid cleaning agent.

2. EXPERIMENTAL

2.1 Materials

Q235 steel was usually used to manufacture mechanical parts, supports, and bogies of high-speed railway trains. In this work, Q235 steel was purchased from the local dealer. The work area used for electrochemical tests was $1 \times 1 \text{ cm}^2$, and the other sides of the Q235 steel block were sealed by epoxy resin. The cleaning agent was also purchased from the local dealer, and the concentration of oxalic acid was 15%, while the thiourea concentration was 20%. To further explore the effect of thiourea, the cleaning agent was diluted, containing 5%, 10%, 15%, and 20% thiourea. The blank test solution was 15% oxalic acid.

2.2 Electrochemical tests

Based on the traditional three-electrode system, the electrochemical experiments were tested. The three-electrode system consisted of the working electrode (1 cm^3 Q235 steel block), saturated calomel electrode with salt bridge, platinum electrode (4 cm^2 platinum sheet). All electrochemical experiments were performed on the same CHI 760E station to ensure results consistency. Firstly, we immersed the electrode in the test solution for a while to obtain a steady state, which was called the self-corrosion potential test. After that, the EIS test was performed from 10^5 to 10^{-2} Hz frequency range with a 5 mV sinusoidal disturbance. In order to detect the current density variation of the steel surface, the potentiodynamic polarization curve test was also carried out when the EIS test was finished. The test potential value was $\pm 250 \text{ mV}$ VS self-corrosion potential, and the scanning rate was 1 mV/s. All electrochemical tests were executed on an electro-thermostatic water bath, and the experimental temperature was controlled at $25 \text{ }^\circ\text{C}$.

2.3 Surface characterization

SEM was employed to observe steel corrosion degree in different test solutions visually. The Q235 steel blocks polished with sandpaper (400 to 7000 mesh) were soaked in the test solution before SEM observation. After being immersed in the test solution for 6 h, the steel sample was washed with deionized water and absolute ethanol. After that, the steel sample was dried via nitrogen gas. The whole observation process was performed under the high vacuum condition via SEM (ZEISS-Gemini-500).

2.4 Calculation details

All computational process of the thiourea molecule in this work was done by dmol software [16, 17]. The geometry optimization of the thiourea molecule was optimized by GGA/BLYP method at the DFT level [18]. Then, Mulliken charge, electrostatic potential (ESP), the highest occupied molecular orbital (HOMO), and the lowest unoccupied molecular orbital (LUMO) were performed [19]. The interfacial state between thiourea molecule and Q235 steel at the molecular level was explored based on the Forcite module of molecular dynamics method. The size of the emulation box was $27.6 \times 17.4 \times 75.6$ Å, which contained 6 layers of frozen Fe (110), 1 thiourea molecule, and 300 H₂O. This box was performed under the COMPASS force field and periodic boundary conditions. The simulation was 200 ps under NVT canonical ensemble [20].

3. RESULTS AND DISCUSSION

3.1 EIS analysis

The EIS results of Q235 steel in different oxalic acid cleaning agent concentrations were studied, and corresponding Nyquist plots were shown in Fig. 2.

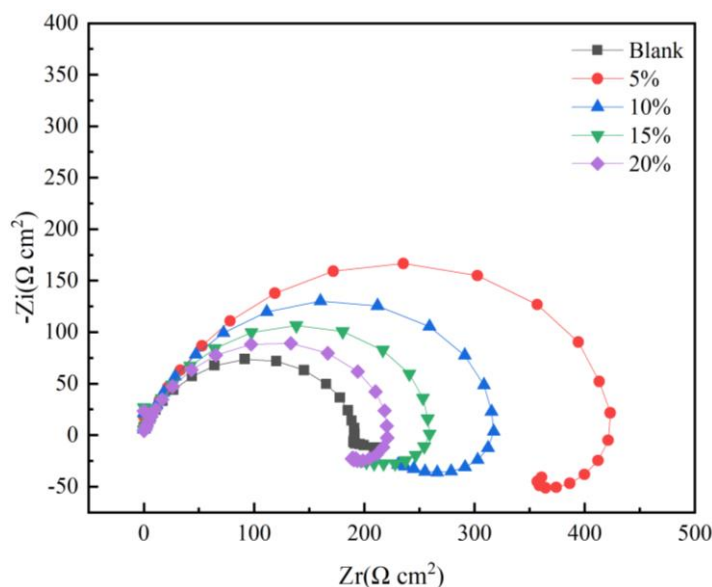


Figure 2. EIS curves of Q235 steel in 15% oxalic acid solution with different concentrations of thiourea (5%、10%、15%、20%) at 298K.

Compared with the blank oxalic acid solution, the radius of the capacitive arc of Q235 steel increased after adding the oxalic acid cleaning agent, which indicated that thiourea could increase the difficulty of oxalic acid reacting on Q235 steel surface and reduce the corrosion rate of Q235 steel.

Meanwhile, this protective phenomenon became apparent with increasing degree of dilution. When diluted to 5%, the Nyquist plot of Q235 steel was the largest, indicating the best protective effect. That was to say, thiourea molecule could be easily adsorbed on the metal surface and formed a protective film in the 5% oxalic acid cleaning agent [21]. Then, as the oxalic acid cleaning agent concentration increased (10% to 20%), the corresponding acidity also increased. There was no doubt that the amount of thiourea was decreased, and then the corrosion degree of Q235 steel was enhanced. On the other hand, the adsorption rate of thiourea on the Q235 steel surface was lower than the rate of Q235 steel dissolution, which also promoted the corrosion of Q235 steel. When the oxalic acid cleaning agent was introduced, all Nyquist plots showed negative values at low frequencies, signifying inductive reactance [22]. This phenomenon could be attributed to the relatively rough electrode surface, the adsorption of corrosive ions on the electrode surface, and the untight protective film formed by thiourea molecules [23-25].

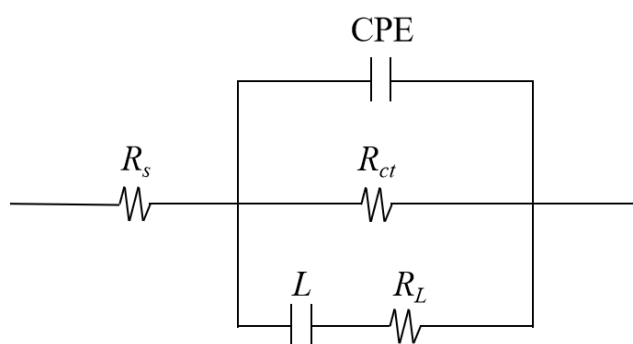


Figure 3. The corresponding equivalent circuits used to fit the original EIS data.

For an in-depth analysis of the EIS results, the original data were fitted by Zsimpwin software. The equivalent circuit used for fitting was given in Fig. 3, and the corresponding fitting results were listed in Table 1. As shown in Fig. 3, R_s was solution resistance, R_{ct} was charge-transfer resistance, CPE was electrical double-layer capacitance.

Table 1. EIS parameters of Q235 steel in 15% oxalic acid solution with different concentrations of thiourea (5%、10%、15%、20%) at 298K.

$C(\%)$	$R_f(\Omega \text{ cm}^2)$	$R_{ct}(\Omega \text{ cm}^2)$	$CPE(\Omega^{-1}\text{s}^n\text{cm}^{-2})$
Blank	1.2	187.2	5.37×10^{-3}
5%	5.7	451.7	1.04×10^{-5}
10%	3.9	329.1	9.22×10^{-5}
15%	5.3	269.1	1.07×10^{-4}
20%	2.8	231.4	1.09×10^{-3}

Based on Table 1, some important parameters such as R_{ct} and CPE were discussed. The R_{ct} value of 5% oxalic acid cleaning agent was the highest and reached $451.7 \Omega \text{ cm}^2$. As the degree of dilution decreased, the value of R_{ct} also decreased. When the oxalic acid cleaning agent concentration was 20%, the R_{ct} value was $231.4 \Omega \text{ cm}^2$. The decrease in the value of R_{ct} indicated that high concentrations of oxalic acid cleaning agent were more likely to corrode the metal and reduced the difficulty of transferring charges on the metal surface [26]. In other words, the lower the oxalic acid cleaning agent concentration, the more pronounced the protection of the metal. The same trend was also shown in the value of CPE . The CPE value of 20% cleaning agent oxalic acid was $1.09 \times 10^{-3} \Omega^{-1} \text{ s}^n \text{ cm}^{-2}$, while the 5% oxalic acid cleaning agent was $9.22 \times 10^{-5} \Omega^{-1} \text{ s}^n \text{ cm}^{-2}$. The 5% oxalic acid cleaning agent value was two orders of magnitude smaller than 20% cleaning agent oxalic acid, which indicated a low concentration of oxalic acid cleaning agent possessed a better corrosion inhibition effect. Meanwhile, a low concentration of oxalic acid cleaning agent also facilitated the adsorption of thiourea on the metal surface [27, 28].

3.2 Potentiodynamic polarization

The Tafel polarization curves of the Q235 steel in the different cleaning agent concentrations (5%, 10%, 15%, and 20%) were shown in Fig. 4.

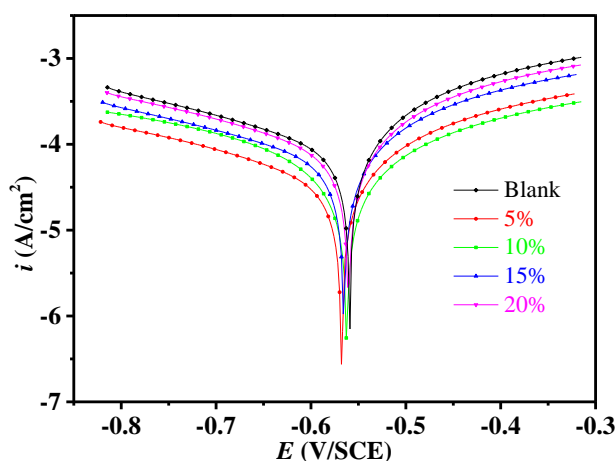


Figure 4. Potentiodynamic polarization curves of Q235 steel in 15% oxalic acid solution with different concentrations of thiourea (5%、10%、15%、20%) at 298K.

With the increase of oxalic acid cleaning agent concentration, the cathodic and anodic curves of Tafel shifted upward, which indicated that the corrosion of the metal was promoted [29]. Especially when oxalic acid cleaning agent concentration was 20%, the corrosion current was the largest and the most serious corrosion phenomenon. Under such conditions, it was difficult for thiourea to provide efficient protection for Q235 steel in oxalic acid solution. When the concentration of oxalic acid cleaning agent was 5%, the whole Tafel polarization curve shifted down obviously, which indicated that enough thiourea molecules effectively suppressed both the cathodic and anodic reactions [30].

Table 2. The polarization parameters of Q235 steel in 15% oxalic acid solution with different concentrations of thiourea (5%、10%、15%、20%) at 298K.

<i>C</i> (%)	E_{corr} (mV/SCE)	β_a (mV dec ⁻¹)	β_c (mV dec ⁻¹)	i_{corr} (μA cm ⁻²)
Blank	-562	72	-113	48.3
5%	-568	76	-116	15.5
10%	-568	76.	-109	25.7
15%	-561	75	-110	32.2
20%	-559	75	-114	37.8

To obtain a deeper catch on the degree of polarization of the cathode and anode, a series of important parameters were analyzed by extrapolation (making a tangent on the cathodic and anodic branches of the Tafel curve and finally intersecting the two tangent lines at the same point). Based on the extrapolation, E_{corr} , β_a , β_c , and i_{corr} were obtained and discussed carefully. As shown in Table 2, the i_{corr} value of Q235 steel was enhanced with the increased concentration of oxalic acid cleaning agent, implying the corrosion rate of Q235 steel has been increased [31]. The corrosion potential was decreased with the increasing dilution. However, the max change of Q235 steel corrosion potential was 9 mV, much less than 85 mV, indicating thiourea was the modest and mixed organic corrosion inhibitor [32]. Meanwhile, the value of β_a and β_c did not significantly change when introduced oxalic acid cleaning agent, indicating that thiourea did not change the reaction mechanism of steel [33]. That was to say, the anti-corrosion mechanism of thiourea for steel was the same under different concentrations [34]. Compared with four oxalic acid cleaning agent concentrations, the 5% possessed the lowest i_{corr} value (15.5 μA cm⁻²), corresponding to the highest anti-corrosion ability. The Tafel results were consistent with EIS, demonstrating the corrosion inhibition performance of thiourea.

3.3 SEM observation

The SEM of new polished Q235 steel and immersed in different oxalic acid solutions (blank, with 5%, 10%, 15% 20% cleaning agent) Q235 steel samples were shown in Fig. 5.

As seen in Fig. 5a, the new polished Q235 steel surface was smooth and shiny; only some scratches after sanding could be seen. Many fluffy corrosion products appeared on the steel surface after being immersed in blank oxalic acid for 6 h. This phenomenon showed that Q235 steel was difficult to resist the corrosion of oxalic acid. Compared with Figs. 5d, e, and f, the corrosion products in Fig. 5c (immersed in 5% cleaning agent) were more dense and fine, which meant that sufficient thiourea molecules could be adsorbed on the metal surface, and thus further form a protective film to inhibit the metal corrosion. In addition, the corrosion of metal also increased with the enhancement of the cleaning

agent concentration, especially when the concentration of the cleaning agent was 20%. This was also consistent with the above electrochemical results that 5% oxalic acid cleaning agent possessed the best anti-corrosion effect, while 20% oxalic acid cleaning agent had the worst effect.

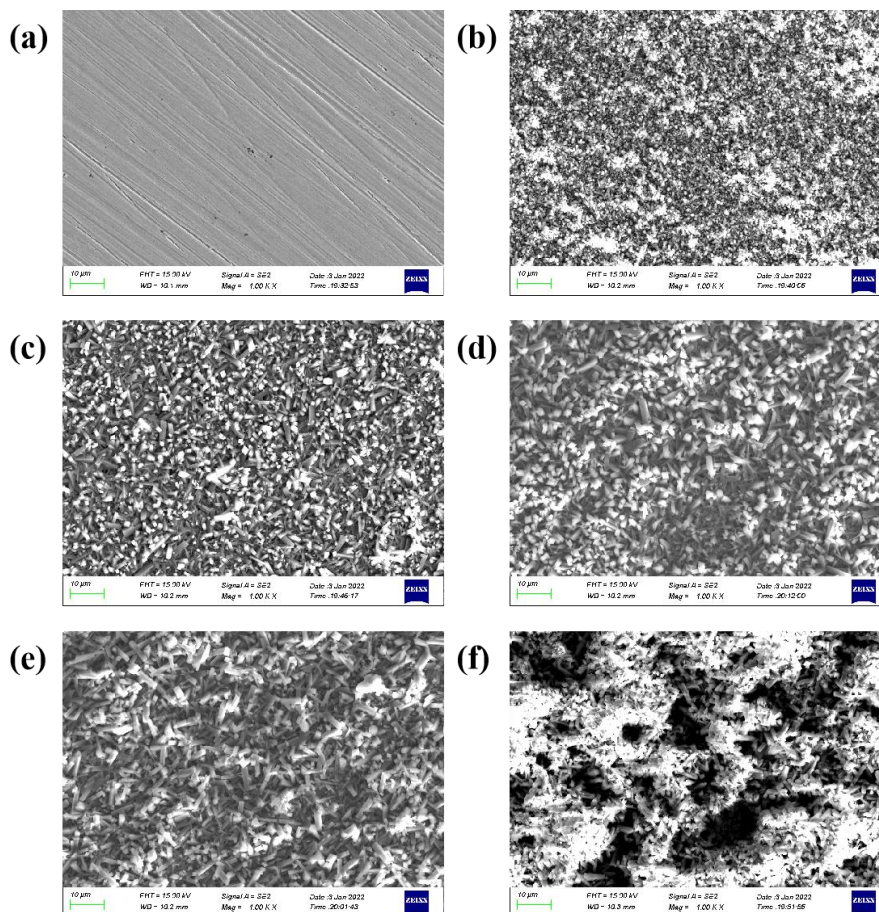


Figure 5. SEM of different Q235 steel samples at 298 K, (a) new polished, (b) blank oxalic acid solution, (c) with 5% cleaning agent, (d) with 10% cleaning agent, (e) with 15% cleaning agent, (f) with 20% cleaning agent.

3.4 Theoretical calculation

Theoretical calculation was a common tool to reveal the interactions between organic corrosion inhibitor molecule and metal interface at the microscopic level. The optimized geometry structure of the thiourea molecule was shown in Fig. 6.

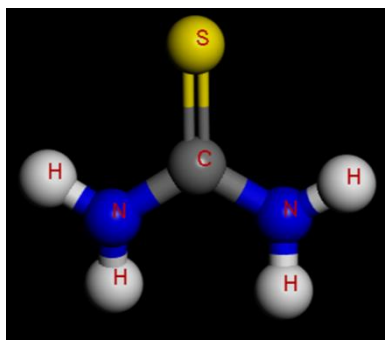


Figure 6. The optimized geometry structure of thiourea molecule.

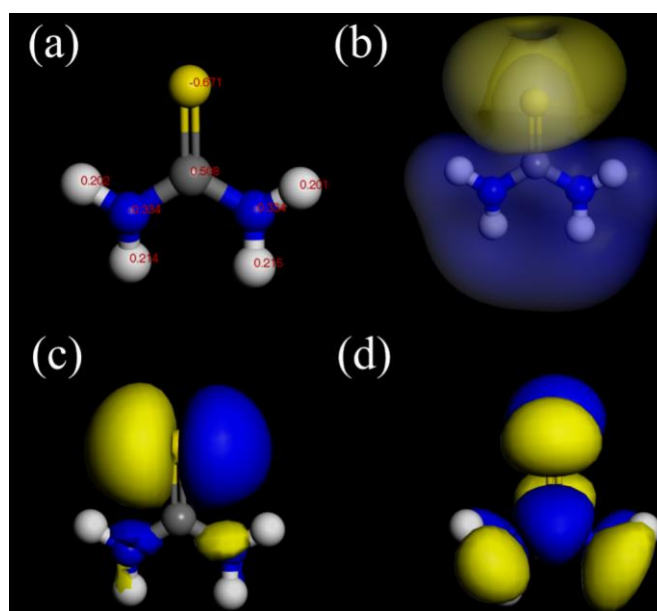


Figure 7. The (a) Mulliken charge, (b) ESP, (c) HOMO, and (d) LUMO of thiourea molecule.

There was no doubt that all atoms in a thiourea molecule were in the same plane, which indicated thiourea molecule possessed the smallest steric hindrance and could easily adsorb on the metal surface. It could be found in Mulliken charge (Fig. 7a) that the charge values of C (0.508) and H atoms (about 0.21) were positive numbers, while the charge values of S (-0.671) and N atoms (-0.334) were negative numbers. That was to say, thiourea molecules could interact with the Q235 steel surface through S and N atoms, especially after the metal was corroded to generate Fe^{2+} . While from the ESP in Fig. 7b, it could be seen that the negative region (yellow area), which corresponded to nucleophilic reactivity, was mainly concentrated on the S atom in the thiourea molecule [35]. The positive region (blue area) was distributed over other atoms in the thiourea molecule. This finding indicated that the S atom, as the active site (engine) in the thiourea molecule, could effectively promote the adsorption of the thiourea molecule on the metal surface. The electron clouds distribution of HOMO and LUMO were displayed in Figs. 7c and d. Clearly, the S atom was covered by the HOMO electron cloud, while the LUMO cloud was

distributed over the entire thiourea molecule. These phenomena indicated that the thiourea molecule could adsorb on the metal surface by exchanging electrons with the metal surface [36].

The HOMO and LUMO values represented the given electrons and obtained electrons ability, respectively. The highest HOMO value stood for the strongest donated electrons ability, while the lowest LUMO value meant the highest gained electrons performance [37]. Moreover, a lower energy gap ($\Delta E = E_{LUMO} - E_{HOMO}$) represented the higher absorption ability and thus corresponded to a supreme anti-corrosion performance [38]. In this work, the E_{LUMO} was -0.92 V, and E_{HOMO} was -4.81 V. Hence the energy gap was 3.89 V, which stood for the high adsorption activity and was polarizable. The dipole moment value (μ) was another parameter to evaluate the corrosion inhibition performance of organic molecules, and the high μ value meant strong anti-corrosion ability [39]. In this work, the μ value was 7.02 Debye, which was much higher than other reports and implied a stronger anti-corrosion ability.

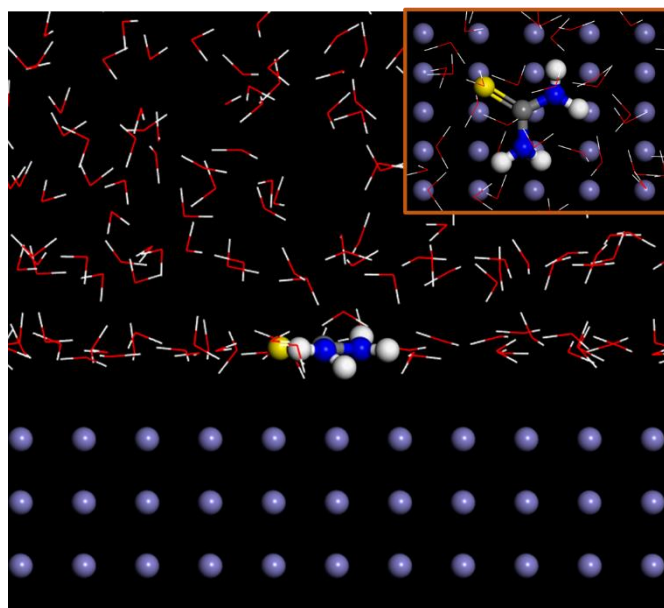


Figure 8. The interface interaction simulation between thiourea molecule and Fe (110).

MD was employed to further explore the interaction between the thiourea molecule and the Q235 steel surface at the micro-level. As shown in Fig. 8, the thiourea molecule parallel adsorption on the Fe (110) lattice plane, which could minimize the contact of corrosive ions with the metal surface. Then, a protective film composed of thiourea molecules was formed on the steel surface, which could facilitate the physicochemical interaction between the thiourea molecules and the steel surface via the gaining and giving electrons.

Based on other reports, we knew that the higher $E_{binding}$ value meant stronger adsorption capacity between organic molecule and metal surface [40, 41]. In this work, the $E_{binding}$ value of thiourea and Fe (110) was higher and reached -55.3 Kcal/mol, indicating the high-efficiency adsorption capacity and supreme anti-corrosion properties of the thiourea molecule.

4. CONCLUSION

This study explored the corrosion inhibition performance of a high-speed trains cleaning agent (with thiourea) for Q235 steel. The dilution degree of high-speed train cleaning agent (with thiourea) was 5%, 10%, 15%, 20%. The main conclusions were as follows:

1. EIS results demonstrated that the high-speed train cleaning agent (with thiourea) could effectively inhibit the corrosion of Q235 steel. When the dilution was 5%, the corrosion inhibition effect was the best.

2. Based on Potentiodynamic polarization curves, it could find that thiourea was a modest and mixed corrosion inhibitor. In addition, thiourea could significantly inhibit the cathodic and anodic reactions of Q235 steel in oxalic acid.

3. In Mulliken charge, ESP, and FMO calculation, we found that S and N atoms in thiourea molecule were the active adsorption sites, which could promote the adsorption of thiourea on the metal surface.

4. The favorable interaction relationship of thiourea and Q235 steel was demonstrated via MD. Meanwhile, MD results also explain the supreme anti-corrosion ability of thiourea at the molecular level.

References

1. E. A. Flores-Frias, V. Barba, M.A. Lucio-Garcia, R. Lopez-Cecenes, J. Porcayo-Calderon, J.G. Gonzalez-Rodriguez, *Int. J. Electrochem. Sci.*, (2019) 5026-5041.
2. M. Cui, J. Dong, K. Zhou, Y. Fang, J. Pu, H. Zhao, Y. Wang, L. Wang, *Int. J. Electrochem. Sci.*, (2018) 12010-12023.
3. L. Guo, S. Kaya, I.B. Obot, X. Zheng, Y. Qiang, *J. Colloid Interf. Sci.*, 506 (2017) 478-485.
4. Y. Qiang, L. Guo, H. Li, X. Lan, *Chem. Eng. J.*, 406 (2021) 126863.
5. B. Tan, B. Xiang, S. Zhang, Y. Qiang, L. Xu, S. Chen, J. He, *J. Colloid Interf. Sci.*, 582 (2021) 918-931.
6. H. Li, Y. Qiang, W. Zhao, S. Zhang, *Colloid. Surf. A*, 616 (2021) 126077.
7. P. Mourya, S. Banerjee, M.M. Singh, *Corros. Sci.*, 85 (2014) 352-363.
8. M.A. Bedair, M.M.B. El-Sabbah, A.S. Fouda, H.M. Elaryian, *Corros. Sci.*, 128 (2017) 54-72.
9. C. Machado Fernandes, V.G.S.S. Pina, L.X. Alvarez, A.C.F. de Albuquerque, F.M. dos Santos Júnior, A.M. Barrios, J.A.C. Velasco, E.A. Ponzio, *Colloid. Surf. A*, 599 (2020) 124857.
10. B. Tan, S. Zhang, H. Liu, Y. Guo, Y. Qiang, W. Li, L. Guo, C. Xu, S. Chen, *J. Colloid. Interf. Sci.*, 538 (2019) 519-529.
11. H. Li, S. Zhang, Y. Qiang, *J. Mol. Liq.*, 321 (2021) 114450.
12. A. Dehghani, G. Bahlakeh, B. Ramezanzadeh, M. Ramezanzadeh, *J. Mol. Liq.*, 277 (2019) 895-911.
13. D.A. Winkler, M. Breedon, P. White, A.E. Hughes, E.D. Sapper, I. Cole, *Corros. Sci.*, 106 (2016) 229-235.
14. Y. Qiang, H. Li, X. Lan, *J. Mater. Sci. Technol.*, 52 (2020) 63-71.
15. C.M. Fernandes, L.X. Alvarez, N.E. dos Santos, A.C. Maldonado Barrios, E.A. Ponzio, *Corros. Sci.*, 149 (2019) 185-194.
16. M.T. Majd, M. Ramezanzadeh, B. Ramezanzadeh, G. Bahlakeh, *J. Hazard. Mater.*, 382 (2020) 121029.
17. Z. Xiao, Z. Zhou, L. Song, D. Wu, C. Zeng, Z. Cao. *Int. J. Electrochem. Sci.*, 14 (2019) 4705-4717.

18. S. Xu, W. Li, X. Zuo, D. Zheng, X. Zheng, S. Zhang, *Int. J. Electrochem. Sci.*, 14 (2019) 5777-5793.
19. J. Zhang, H. Li, *Int. J. Electrochem. Sci.*, 15 (2020) 5362-5372.
20. Z. Zhang, N. Tian, W. Zhang, X. Huang, L. Ruan, L. Wu, *Corros. Sci.*, 111 (2016) 675-689.
21. X. Zheng, S. Zhang, W. Li, M. Gong, L. Yin, *Corros. Sci.*, 95 (2015) 168-179.
22. Y.Z. Li, N. Xu, G.R. Liu, X.P. Guo, G.A. Zhang, *Corros. Sci.*, 112 (2016) 426-437.
23. D. Daoud, T. Douadi, S. Issaadi, S. Chafaa, *Corros. Sci.*, 79 (2014) 50-58.
24. Y. Qiang, H. Zhi, L. Guo, A. Fu, T. Xiang, Y. Jin, *J. Mol. Liq.*, 351 (2022) 118638.
25. X. Li, S. Deng, H. Fu, *Corros. Sci.*, 53(1) (2011) 302-309.
26. L. Guo, S. Zhu, S. Zhang, Q. He, W. Li, *Corros. Sci.*, 87 (2014) 366-375.
27. I.B. Onyeachu, I.B. Obot, A.A. Sorour, M.I. Abdul-Rashid, *Corros. Sci.*, 150 (2019) 183-193.
28. H. Li, Y. Qiang, W. Zhao, S. Zhang, *Corros. Sci.*, 191 (2021) 109715.
29. Y. Qiang, S. Zhang, B. Tan, S. Chen, *Corros. Sci.*, 133 (2018) 6-16.
30. H. Qian, D. Zhang, Y. Lou, Z. Li, D. Xu, C. Du, X. Li, *Corros. Sci.*, 145 (2018) 151-161.
31. Y. Qiang, S. Zhang, H. Zhao, B. Tan, L. Wang, *Corros. Sci.*, 161 (2019) 108193.
32. Y. Qiang, S. Fu, S. Zhang, S. Chen, X. Zou, *Corros. Sci.*, 140 (2018) 111-121.
33. H. Li, S. Zhang, B. Tan, Y. Qiang, W. Li, S. Chen, L. Guo, *J. Mol. Liq.*, 305 (2020) 112789.
34. Z. Sanaei, G. Bahlakeh, B. Ramezanzadeh, M. Ramezanzadeh, *J. Mol. Liq.*, 290 (2019) 111176.
35. M. Ramezanzadeh, G. Bahlakeh, Z. Sanaei, B. Ramezanzadeh, *J. Mol. Liq.*, 272 (2018) 120-136.
36. M. Ramezanzadeh, Z. Sanaei, G. Bahlakeh, B. Ramezanzadeh, *J. Mol. Liq.*, 256 (2018) 67-83.
37. D.K. Verma, A. Al Fantazi, C. Verma, F. Khan, A. Asatkar, C.M. Hussain, E.E. Ebenso, *J. Mol. Liq.*, 314 (2020) 113651.
38. A. Dehghani, G. Bahlakeh, B. Ramezanzadeh, M. Ramezanzadeh, *J. Taiwan Inst. Chem. Eng.*, 100 (2019) 239-261.
39. A. Singh, K.R. Ansari, Y. Lin, M.A. Quraishi, H. Lgaz, I.-M. Chung, *J. Taiwan Inst. Chem. Eng.*, 95 (2019) 341-356.
40. J. Haque, V. Srivastava, C. Verma, H. Lgaz, R. Salghi, M.A. Quraishi, *New J. Chem.*, 41(22) (2017) 13647-13662.
41. R. Farahati, S.M. Mousavi-Khoshdel, A. Ghaffarinejad, H. Behzadi, *Pro. Org. Coat.*, 142 (2020) 105567